JOURNAL OF SOLID STATE CHEMISTRY 71, 503–512 (1987)

Defect Intergrowths in Barium Polytitanates

2. $BaTi_5O_{11}$

PETER K. DAVIES AND ROBERT S. ROTH*

*Department of Materials Science and Engineering, University of Pennsylvania, Philadelphia, Pennsylvania 19104; and *National Bureau of Standards, Gaithersburg, Maryland*

Received May 6, 1986; in revised form April 16, 1987

High resolution electron microscopy has been used to investigate the structure of $BaTi_5O_{11}$. Single-phase materials were prepared from alkoxide precursors and studied using lattice imaging and microdiffraction techniques. Considerable structural disorder was observed in all the samples investigated. In general, isolated defects were observed. These resulted from a displacement of the close-packed layers of the structure giving some face-sharing of the Ti octahedra. However, in several regions of the samples, systematic stacking faults lead to the formation of a new polytypic structure. The paper describes the defect mechanisms, and relates these to the structure of the new polytype.

1. Introduction

In our continuing investigation of phases in the $BaTiO_3$–TiO_2 system we report here our results of a study of $BaTi_5O_{11}$. Until recently (*1*), this phase was only obtained metastably from the melt (*2*), or was observed as an intermediate reaction product (*3*). However, phase studies using alkoxide precursors have shown that the 1:5 material can be prepared as a single phase at temperatures up to 1130°C (*1*). The phase diagram as determined from the alkoxide precursor technique is reproduced in Fig. 1.

Many of the barium polytitanates have dielectric properties suited toward their use as ceramic resonators in microwave filters. $Ba_2Ti_9O_{20}$ and $BaTi_4O_9$ are used commercially in the communications industry. The impetus for preparation of a single-phase $BaTi_5O_{11}$ ceramic resulted from the variation of the dielectric properties across the $BaTiO_3$–TiO_2 system. Experimental values for the dielectric constant K, the dielectric loss Q, and the temperature coefficient of the dielectric constant τ_K at microwave frequencies were determined by O'Bryan (*4*) and are shown in Fig. 2. Extrapolation of these to the $BaTi_5O_{11}$ composition indicates this material should have a τ_K close to zero, thus making this ceramic an extremely attractive candidate for use in the resonator devices.

Crystallographically, $BaTi_5O_{11}$ is similar to most of the phases in the $BaTiO_3$–TiO_2 system. Its structure can be described in terms of a close-packed array of oxygen and barium ions, with Ti occupying appropriate octahedral interstices (*2*). The struc-

0022-4596/87 $3.00

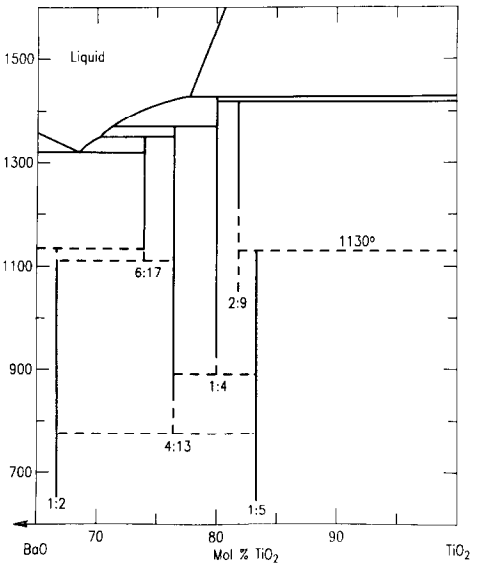

FIG. 1. Phase diagram constructed from data obtained from heat treatments of specimens obtained from hydrolysis of alkoxide precursors (from Ref. (*1*)).

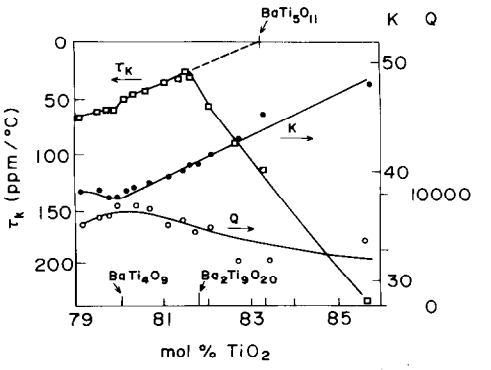

FIG. 2. Variation of the dielectric loss Q, the dielectric constant K, and the temperature coefficient of the dielectric constant τ_K, with mole percent TiO_2 (data from Refs. (*1*) and (*3*)).

ture consists of a six-layer ABCACB stacking sequence, the same as that found in $BaTiO_3$ (*5*), $Ba_4Ti_{13}O_{30}$ (*6*), and $Ba_2Ti_{9.25}Li_3O_{22}$ (*7*). The unit cell is monoclinic, space group $P2_1/n$, with $a = 0.767$ nm, $b = 1.402$ nm, $c = 0.752$ nm, $\beta = 98.33$. A schematic of the atomic arrangements in each of the six layers of the structure is shown in Fig. 3. There is no face-sharing of Ti octahedra but only edge- and corner-sharing. Two of the close-packed layers, at $y = \frac{1}{6}$ and $\frac{4}{6}$, are occupied solely by oxygen, the remainder contain one barium and seven oxygens. The formal compositions of each layer and the associated octahedral ions below it are, $BaTi_2O_7^{4-}$, Ti_4O_8, $BaTi_4O_7^{4+}$, $BaTi_2O_7^{4-}$, Ti_4O_8, and $BaTi_4O_7^{4+}$, respectively.

In this study we have used high resolution TEM to investigate the microstructure of $BaTi_5O_{11}$ ceramics prepared from alkoxide precursors. Apart from an X-ray structural determination of a single crystal grown metastably from a melt (*2*), no other structural studies of this material have been reported in the literature.

2. Sample Preparations

Specimens were examined which had been obtained by heat treatments of powders formed by hydrolysis of metal organic precursors. The technique was fully

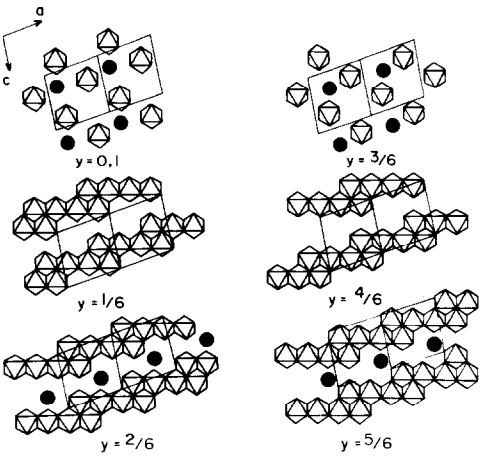

FIG. 3. Schematic of the atomic arrangement in each of the layers of the $BaTi_5O_{11}$ structure. Filled circles represent barium ions; oxygen positions are represented by the corners of the polyhedra surrounding the titanium ions.

described by Ritter *et al.* (*1*) and involved preparation of Ba-ethoxide and Ti-ethoxide solutions. These solutions were mixed in a dry argon atmosphere in the desired proportions and then hydrolyzed with or without refluxing by the dropwise addition of 10:1 ethanol:water. The precipitate formed was centrifuged, filtered, washed, and dried at 110°C. Heat treatments were performed in Au or Pt crucibles in a $MoSi_2$ box furnace for times ranging from 1 hr to several weeks and at temperatures from ≃500°C to the beginning of decomposition of the $BaTi_5O_{11}$ phase above 1100°C. As fully documented in Ref. (*1*) the low temperature precipitation and heat treatment of a precursor solution is the only known way to produce single-phase $BaTi_5O_{11}$ specimens.

3. Experimental

The samples of $BaTi_5O_{11}$ were prepared for microscopy by dispersing on holey carbon grids in the usual manner. Microscopes were used at the University of Pennsylvania and at the National Bureau of Standards. These included a Philips 400T and 430T. Images and diffraction patterns were collected along several different zone axes; however, the [100] zone was found to give the maximum amount of contrast information and was the main orientation used in the high resolution work. Some multislice image calculations of the defect-free structure were performed using computer programs developed at Arizona State, and the SHRLI programs developed by O'Keefe (*8*). Extensive image simulation of defects was not attempted and was outside the scope of this work.

4. Results

Along the [100] zone axis, used most extensively in the high resolution work, we were able to identify both the projected arrangement of the barium positions in each close-packed layer, and the variation in the positions along the stacking direction. A schematic of the projected barium and titanium positions is given in Fig. 4, the oxygen anions have been omitted for clarity. Figure 4 also shows an image calculated at the Scherzer defocus, ≃−70 nm for the 430T, for this orientation. In Fig. 5 we present the corresponding experimental image which confirms the validity of the structural arrangement. However, streaking in the selected area diffraction patterns collected from larger regions of the grain (see inset to Fig. 6) indicated that the

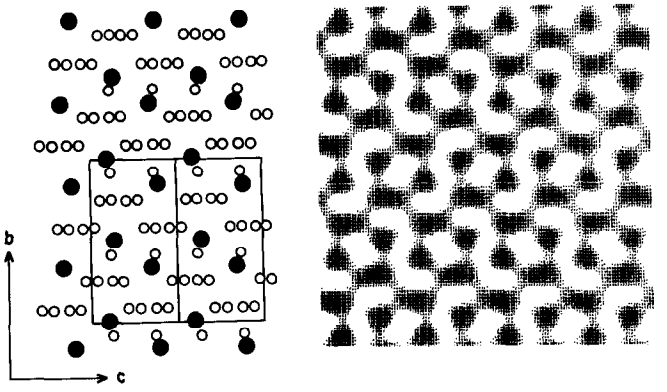

FIG. 4. Schematic of the barium and titanium positions projected along [100]; filled circles, Ba; open circles, Ti; the unit cell is outlined. The corresponding multislice image was calculated at $\Delta f = -70$ nm.

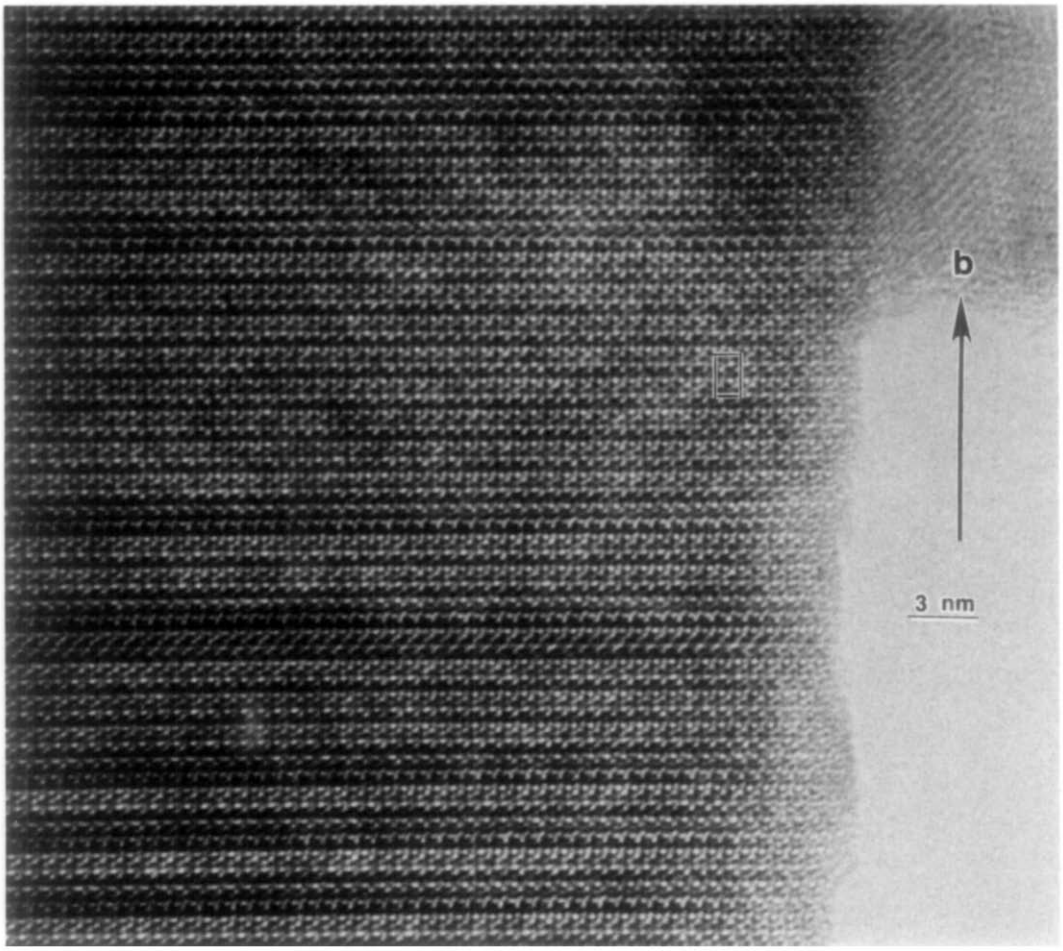

FIG. 5. A high resolution lattice image of $BaTi_5O_{11}$ with the beam along [100]; the unit cell is outlined.

microstructure shows considerable stacking disorder along the b^* direction. A lower resolution image (Fig. 6) confirms the diffraction information and indicates the material is substantially defective. Most of the disorder appears to result from isolated linear defects, but in certain regions of the grain we observed several sequential defects which give rise to several unit cells of a new structure type; see, e.g., Fig. 7. In these regions the contrast from the barium ions in successive close-packed layers lies along a direction at 80° from the c axis.

From the observed contrast variations resulting from the linear stacking faults we have been able to model the defect mechanism. All the defects appear to result from a displacement of certain specific close-packed layers leading to some face-sharing of Ti Octahedra. In order to avoid large-scale structural changes, the rearrangement of the Ti octahedra always occurs by a displacement above the close-packed layers containing only oxygen ions, i.e., those above $y = \frac{1}{6}$ and $y = \frac{4}{6}$. In Fig. 8 we illustrate the face-sharing produced by a displacement of the layer at $y = \frac{2}{6}$ relative to $y = \frac{1}{6}$ by $0.4a$ and $0.16c$. The mechanism

shown results in a minimum number of shared faces, one per unit cell, and no change in the overall stoichiometry. The ABCACB stacking sequence is also unchanged. The same mechanism can also be applied to the layers at $y = \frac{4}{6}$ and $\frac{5}{6}$.

The change in the [100] projected arrangement resulting from these defects is

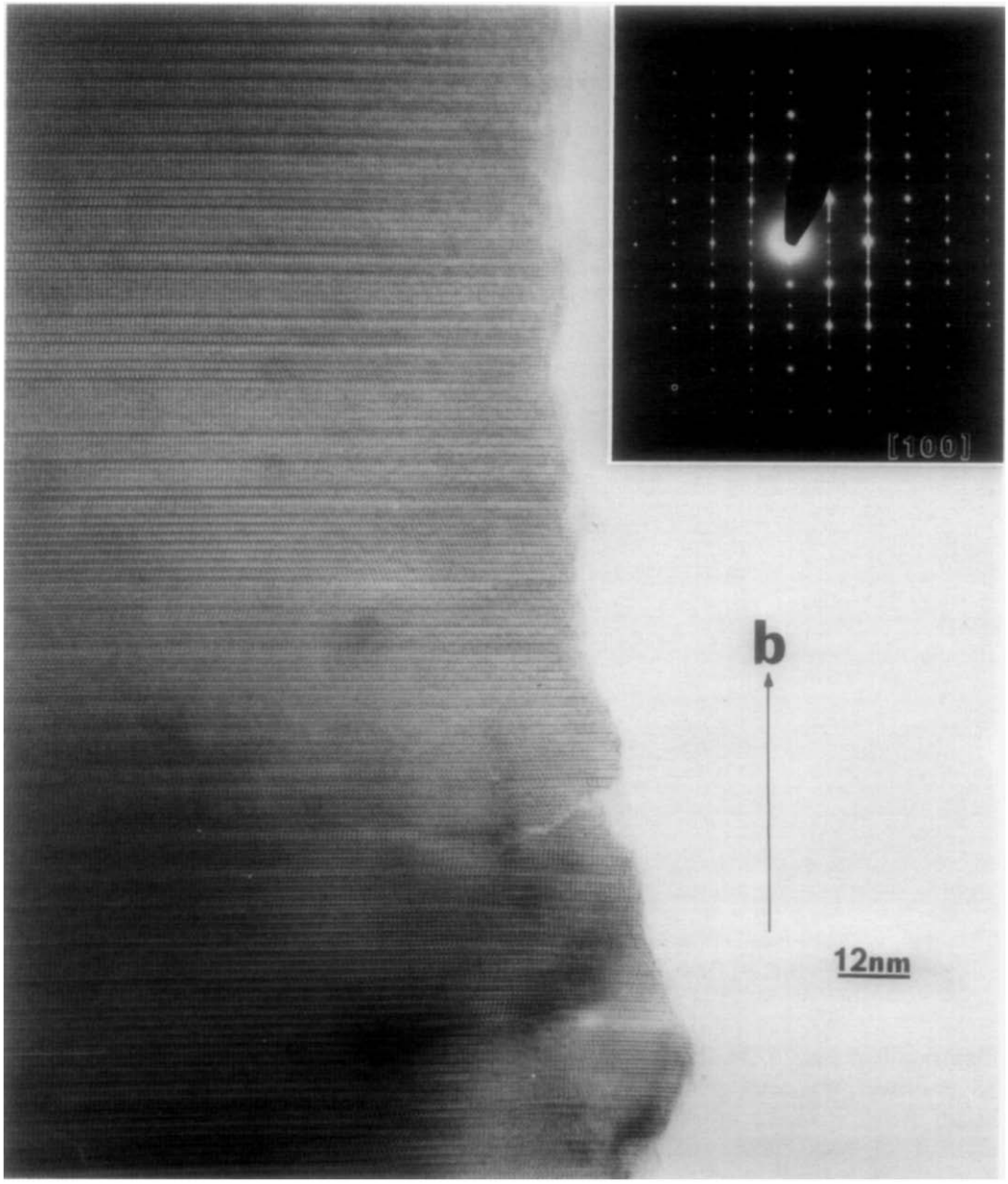

FIG. 6. A lower magnification image and corresponding diffraction pattern illustrating the disorder along *b*.

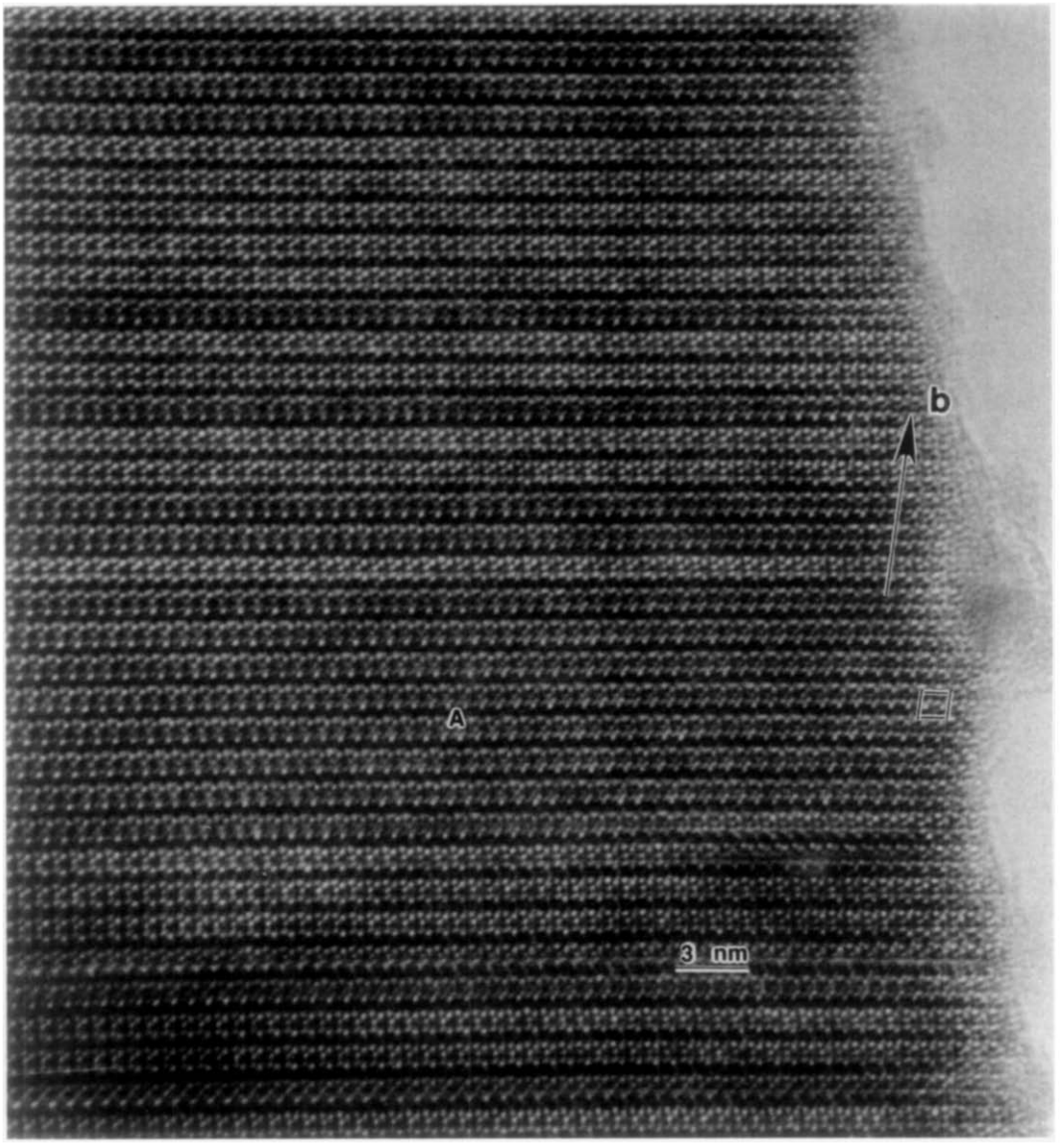

FIG. 7. Lattice image of the new polytype formed in $BaTi_5O_{11}$. In the region labeled A several unit cells of the polytype are coherently intergrown in the matrix.

illustrated in Fig. 9. In this schematic we have drawn the arrangement that would result from a series of displacements at every Ti_4O_8 layer. This structure represents a new polytype of $BaTi_5O_{11}$. The overall structural stacking sequence is the same as that in the original monoclinic cell; however, the angle between the projected *b* and *c* cell axes is no longer 90°. As shown by the schematic this angle is now approximately 80°, in excellent agreement with that observed in the experimental images.

Discrete reflections corresponding to the structure of the new polytype were observed in microdiffraction patterns of grains containing a sizeable fraction of

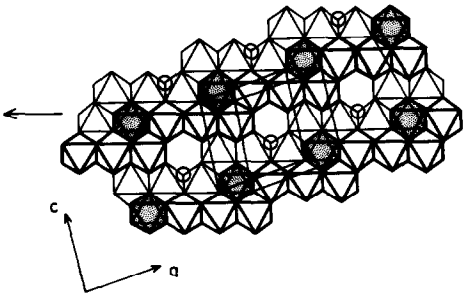

FIG. 8. Displacement of the layer at $y = \frac{3}{8}$, giving face-sharing (shaded octahedra) with the octahedra in the layer below; open circles represent Ba ions.

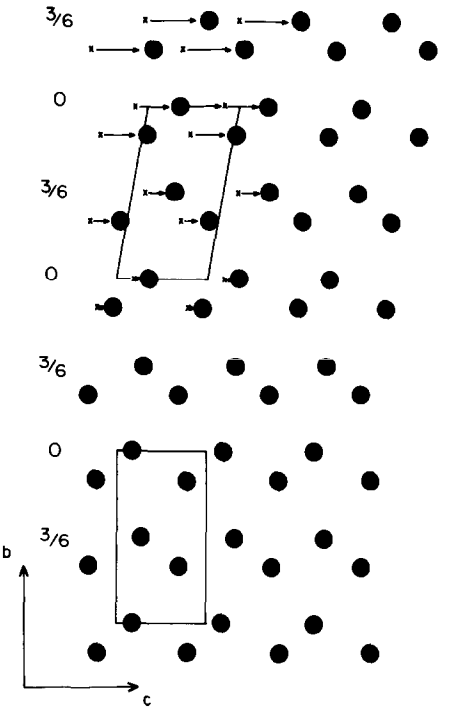

FIG. 9. Schematic showing the displacement of Ba ions to give the new polytype. Ti and O atoms are omitted for clarity; × represents the original Ba positions.

defects. One of these is reproduced in Fig. 10, the weak reflections corresponding to the new structure are arrowed. The accompanying schematic indicates the reflections expected from the 1:5 structure and the new polytype. The experimental pattern is somewhat complicated by the streaking along b^*. However, the reflections along the $(0kl)$ rows with $k = 3n$ are considerably less disordered than the other rows. Reference to the schematic of the expected patterns of the two structures shows that the

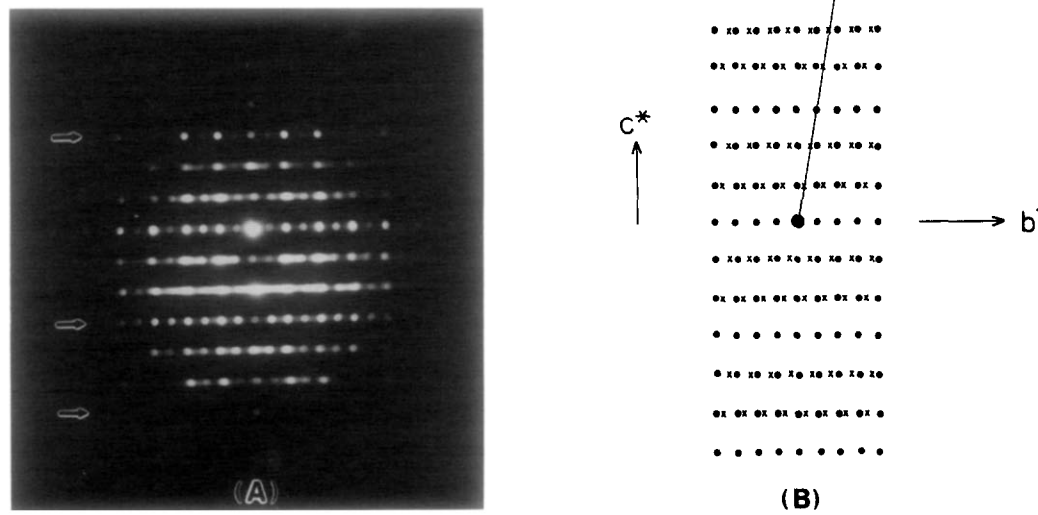

Fig. 10. (A) Microdiffraction pattern from an area containing a large number of intergrowths of the new polytype; the $(0kl)$ rows with $k = 3n$ are arrowed. The additional reflections from the new structure, denoted by ×, are illustrated in the schematic (B).

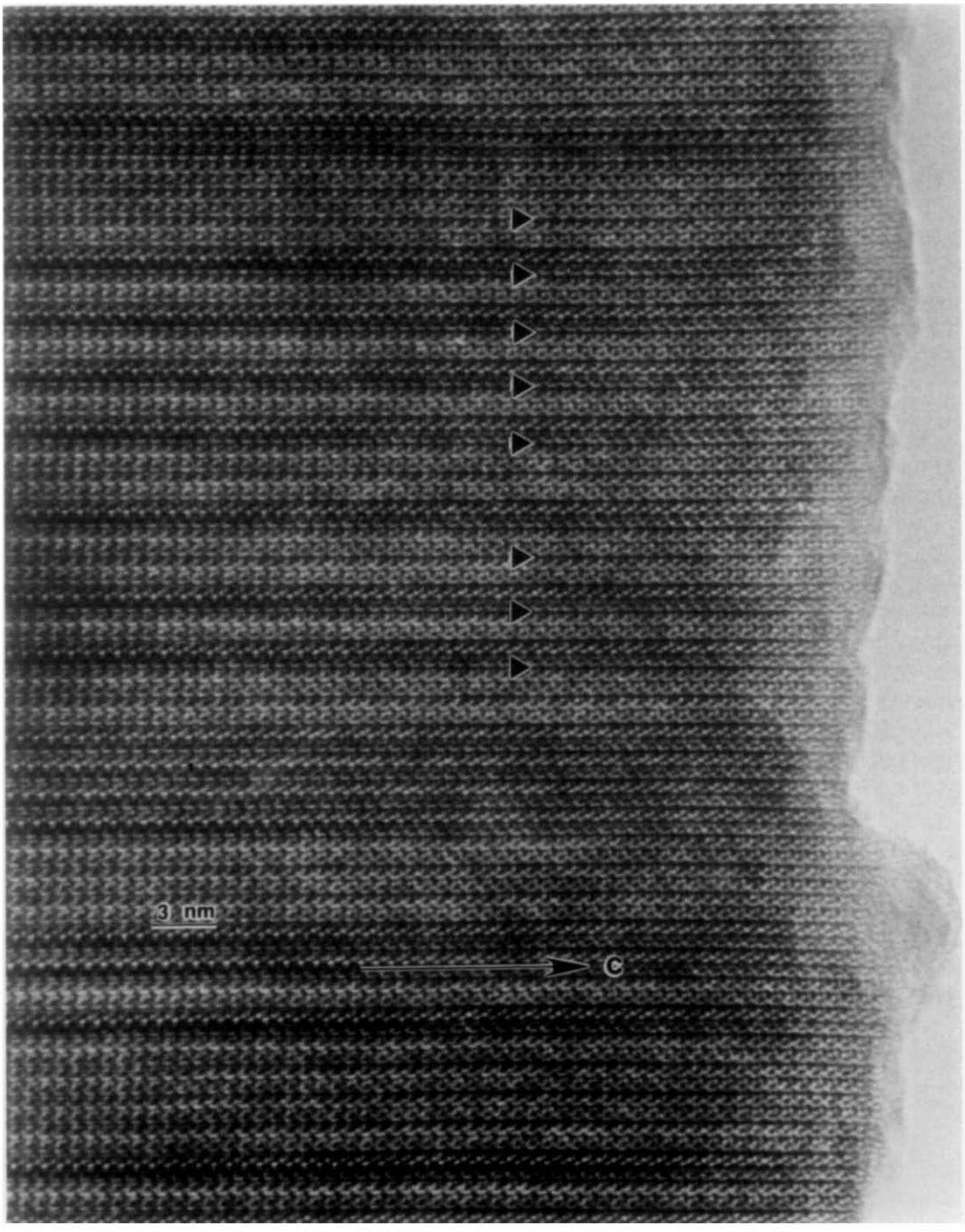

FIG. 11. Formation of long-period superstructures, arrowed, by the intergrowth of the two polytypes.

reflections in these rows superimpose, whereas for $k = 3n$ the additional reflections from the polytype are in different positions to those of the 1 : 5 structure.

Although coherent intergrowths of several unit cells of the new polytype were observed in many regions of the grains, a large fraction of the structural disorder results from isolated linear defects. Extensive long-period superstructure formation caused by systematic unit cell intergrowth of the two polytypes was not generally observed. However, isolated examples were found. For example, in Fig. 11 a sequence consisting of an ordered alternation of one unit cell of each polytype extends over a distance greater than would be expected from a statistical distribution of intergrowths. Correspondingly, weak superlattice reflections corresponding to long-period repeats were occasionally observed in the diffraction patterns.

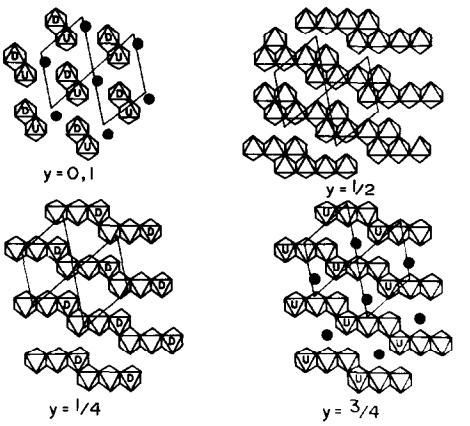

FIG. 12. Schematic of the atomic arrangement in each of the layers of the $BaTi_6O_{13}$ structure; filled circles represent barium ions. D and U represent lower and upper shared faces, respectively.

5. Discussion

In the previous section we described the results and mechanism for defect formation in $BaTi_5O_{11}$. We have observed that this material contains many stoichiometric defects resulting from face-sharing of Ti octahedra. In several cases a regular arrangement of these faults leads to the formation of a new polytype. From a thermodynamic point of view the new structure is necessarily energetically less stable than the original structure because of the "unfavorable" face-sharing. However face-sharing of octahedra does occur in other phases in this system. For example, in the close-packed structure of $BaTi_6O_{13}$ (*9*), substantial face-sharing has been reported. The structure of the close-packed layers in this phase has been calculated from the original data and is shown in Fig. 12. In the four-layer repeat of the unit cell the compositions of the layers at $y = 0$, $\frac{1}{4}$, $\frac{1}{2}$, and $\frac{3}{4}$ are $BaTi_2O_6^{2-}$, $Ti_3O_7^{2-}$, $Ti_4O_7^{2+}$, and $BaTi_3O_6^{2+}$, respectively. The octahedra sharing faces are as shown in the diagram. In this case the unfavorable energetics of face-sharing are exemplified by the extreme difficulty in the preparation of stable one-phase materials. The phase has only been prepared metastably from the melt. Despite the similarity of this structure and that of the two $BaTi_5O_{11}$ polytypes no intergrowths of this phase were observed in our samples.

Although we have found evidence for polytypism in $BaTi_5O_{11}$ this material is not as defective as samples of $Ba_2Ti_9O_{20}$, which are reported in a separate publication (*10*). However, the two materials are similar in that both are defective and the defects result almost exclusively without any change in the overall stoichiometry. Measurements of the dielectric properties of $BaTi_5O_{11}$ are currently being made; it will be interesting to observe the effects of both the defects and the higher titania content, as coefficient of the dielectric constant.

Acknowledgments

This work was supported by NSF, Solid State Chemistry, Grant DMR 831699 (P.K.D.). Use of facil-

ities provided under NSF (M.R.L.) Grant DMR 8216718 (P.K.D.) is also acknowledged.

References

1. J. J. RITTER , R. S. ROTH, AND J. E. BLENDELL, *J. Amer. Ceram. Soc.* **69,** 155 (1986).
2. E. TILLMANNS, *Acta Crystallogr. Sect. B* **25B,** 1444 (1969).
3. H. M. O'BRYAN AND J. THOMSON, *J. Amer. Ceram. Soc.* **58,** 454 (1975).
4. H. M. O'BRYAN, *J. Amer. Ceram. Soc.* **57,** 450 (1974)
5. R. D. BURBANK AND H. T. EVANS, JR., *Acta Crystallogr.* **1,** 330 (1948).
6. E. TILLMANNS, AND W. H. BAUR, *Acta Crystallogr. Sect. B* **26B,** 1645 (1970).
7. E. TILLMANNS AND I. WENDLT, *Z. Kristallogr.* **144,** 16 (1976).
8. M. O'KEEFE AND P. R. BUSECK, *Trans. Amer. Crystallogr. Assoc.* **15,** 27 (1979).
9. E. TILLMANNS, *Crystallogr. Struct. Commun.* **1,** 1 (1972).
10. P. K. DAVIES AND R. S. ROTH, *J. Solid State Chem.* **71,** 490 (1987).